SST Optics:
Design Report

SST-OPT-DSR-001

Version 1a

Prepared by:		
Giorgia Sironi (INAF)	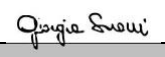	SST-OPT SS
Latest Release Checked by:		
Gino Tosti (INAF)		SST-STR SE
Nicola La Palombara (INAF)	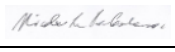	SST-STR PA/QA
Alberto Macchi (INAF)		SST-STR CADM
Approved by:		
Salvatore Scuderi (INAF)		SST-STR PM

Current Release				
Ver.	Created	Comment	Distribution	Editor(s)
1a	25/11/2022		SST Consortium	Giorgia Sironi (INAF)

Version History				
Ver.	Created	Comment	Distribution	Editor(s)
1aD	14/10/2022	Revision of DVER document: 4e SST-STR Description of the Intended Final Design (Optical Description). Implemented DVER RIX #40583, #40584,	SST Consortium	Giorgia Sironi (INAF)

Table of Contents

List of Figures

List of Tables

1 Introduction

1.1 Scope & Purpose

This document describes the optical design adopted for the CTS-SSTs. In section 2 the optical configuration and the optical components description are given. In section 3 we justify the chosen design reporting the optical system performance that are subject to telescope requirements. In section 4 we report the optical system error budget setting the tolerances to be used as requirement for optics implementation.

1.2 CTA-SST General Description

When a VHE gamma-ray interacts with the atoms and ions in the upper levels of the atmosphere, it induces a cascade of secondary particles which propagate over many kilometres at nearly the speed of light through the atmosphere. These particles emit Cherenkov light, forward-beamed with an opening angle of about one degree. A Cherenkov light event consists of a time-correlated multi-photon image with a typical timescale of ~10 ns. Cascades originate at an altitude of ~10 km above ground and create a light pool on the ground of ~120 m radius. Telescopes placed on the ground, containing large reflectors, focus the light to and imaging camera. Such Cherenkov cameras must be highly pixelated, cover a large field of view, and be able to detect UV/blue light down to the single photon levels with exposure times of approximately a billionth of a second. To provide a high imaging sensitivity over an extensive energy range, from a few tens of GeV up to a few hundreds of TeV, the Cherenkov Telescope Array Observatory (CTAO, see web page link at https://www.cta-observatory.org) will be made of sub-arrays with three different types of telescopes: large-sized (LST, 23 m diameter), medium-sized (MST, 12 m diameter) and small-sized (SST, 4 m diameter) telescopes. They are distributed in two observing sites, the Northern one in La Palma, the Canary Islands, and the Southern one in the Chilean Andes in the Paranal area. The CTA South "Alpha Configuration" would include LSTs, MSTs and SSTs. In particular, it envisages the construction and installation of 42 SSTs (a number that could increase up to 70 in future upgrades).

The SSTs are developed by an international consortium of institutes that will provide them as an in-kind contribution to CTAO. The SSTs rely on a Schwarzschild-Couder-like dual-mirror polynomial optical design, with a primary mirror of 4 m diameter, and are equipped with a focal plane camera based on SiPM detectors covering a field of view of ~9°. They are sensitive in the band from ~0.5 TeV up to ~300 TeV, providing the Observatory with sensitivity to the highest energies. The current SST concept has been validated by developing the prototype dual-mirror ASTRI-Horn Cherenkov telescope and the CHEC-S Cherenkov camera. Table 1 reports main properties of the Small-Sized telescope (SST).

Table 0. Small-sized telescope main properties

Small-Sized telescope (SST) main properties:	
Optical Design	modified Schwarzschild-Couder
Primary reflector diameter	4.3 m
Secondary reflector diameter	1.8 m
Effective mirror area (including shadowing)	>5 m2
Focal length	2.15 m
Total weight	17.5 t
Field of view	> 8.8 deg

Number of pixels in SST Camera	2048
Pixel size (imaging)	0.16 deg
Photodetector type	SiPM
Telescope data rates (before array trigger)	> 600 Hz
Telescope data rates (readout of all pixels; before array trigger)	2.6 Gb/s
Positioning time to any point in the sky (>30° elevation)	90 s
Pointing Precision	< 7 arcsecs

1.3 Applicable Documents

[AD1] SST Programme Project Management Plan SST-PRO-PLA-001 Version 1.a
[AD2] SST Configuration Management Plan SST-PRO-PLA-002 Version 1.a
[AD3] Telescope Technical Requirements Specification SST-PRO-SPE-001 Version 1a
[AD4] Subsystem Technical Requirement Specification SST-OPT-SPE-002
[AD5] Design Report SST-OPT-DSR-001

1.4 Reference Documents

[RD1] CTA-SST Engineering Review Panel Report CTA-RER-SST-305000-0001_2aIssue 2, Rev. 0, 2020-09-01
[RD2] SST Engineering Review – DMA Disposition CTA-INS-SST-305000-0001, 2020-11-02
[RD3] Vassiliev V., Fegan S. and Brousseau P., 2007, Astroparticle Phys., 28, 10

1.5 Definition of Terms and Abbreviations

cFOV Camera Field of View
CPM Camera Project Manager
CTA Cherenkov Telescope Array
CTAO Cherenkov Telescope Array Observatory
EE Encircled Energy
FOV Field of View
FS Focal Surface
INAF Istituto Nazionale di Astrofisica
LST Large Size Telescope
M1 Primary Mirror
M2 Secondary Mirror
MST Medium Size Telescope
PSF Point Spread Function
SiPM Silicon Photo Multiplier
SST Small Size Telescope
VHE Very High Energy

2 Optical description

2.1 Introduction

The optical design for the CTA-SST telescopes has been developed by INAF in the framework of the ASTRI project for the realization an end-to-end Cherenkov telescope prototype installed at Serra La Nave Observatory called ASTRI-Horn.

The general idea of the design is to populate the focal plane with detectors of new generation in the field of Cherenkov Astrophysics called Silicon Photomultipliers (SiPMs). These sensors have a linear dimension about 4 times less of the traditional phototubes and this fact implies to propose a new optical design to optimize the PSF in the FoV.

The optical system (OS) design of CTA-SST Telescopes was developed in compliance with the requirements in [AD3] to have a PSF (described by the diametric dimension containing the 80% of the energy - D80) smaller than 0.25° degrees and a geometrical area larger than 5 m^2 across a FOV of at least 8° degrees.

2.2 Optical layout

The optical layout selected for CTA-SST is based on a Schwarzschild Couder configuration (SC) consisting of three optical surfaces represented in figure 1: the primary mirror (M1), the secondary mirror (M2), and the curved focal surface (FS) populated with SiPM sensors.

The design optimization has been done in such a way the amount of energy contained within a physical pixel, hereafter called Cherenkov pixel, is not less than 80% across a 9° degrees field angle. This parameter is named Encircled Energy (EE). The pixel size used for the design is 6.2 mm wide although subsequently a new size of 7 mm will be mounted in the camera of the CTA-SST telescopes

The design has been performed using the commercial software for optical system design ZEMAX.

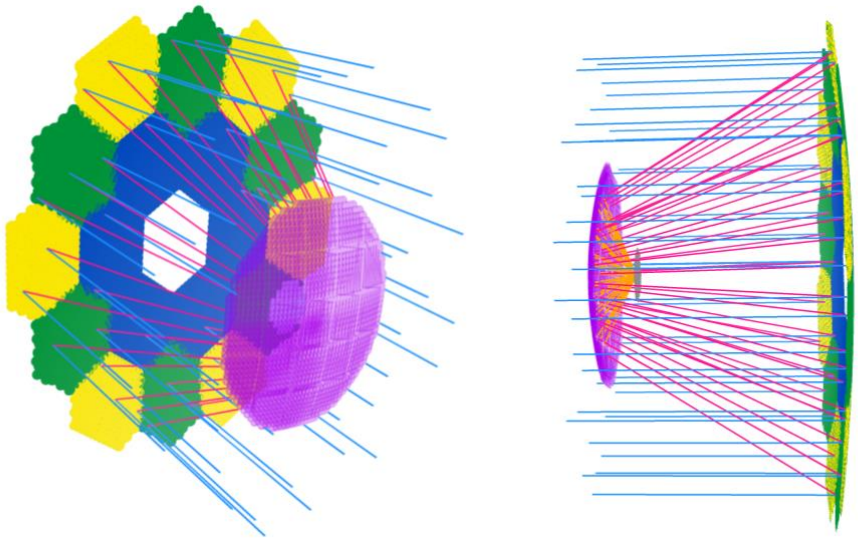

Figure 1 - The Schwarzschild-Couder optical design adopted for CTA-SST. The primary mirror is represented as blue, green and yellow segments. The secondary monolithic mirror is represented in violet and the focal surface in grey.

The effective focal length of the obtained OS is F = 2154 mm. The distance between M1 and M2 is 3108.4 mm = F/q, where q = 0.6888 is the first Schwarzschild aplanat parameter. The distance between M2 and FS is 519.6 mm = F (1 − α), where α = 0.7573 is the second parameter, which together with q defines the Schwarzschild aplanatic solution. It has been shown in [RD3] that the optical systems in the vicinity of q = 2/3 and α = 2/3 are nearly optimal for applications in ground-based gamma-ray astronomy. The aperture of the CTA-SST is D = 4306 mm, which makes its OS very fast, with F/D = 0.50. The other OS parameters are summarized in Table 1.

Table 1 - Optical system main dimensions

ELEMENT NAME	DIAMETER [mm]	RADIUS OF CURVATURE [mm]	SHAPE	DISTANCE TO [mm]
M1	4306	-8223	Even asphere	M2: 3108.4
M2	1800	2180	Even asphere	DET: 519.6
FS	(side) 360	1060	Spherical	--

2.3 Optical layout polynomial optimization

The OS of CTA-SST was designed to provide correction of aberrations within the full camera field of view by polynomial optimization of the SC configuration.

Hence the sag z of each of the three optical surfaces of the OS was parameterized by a spherical term and the conical constant (describing the SC system) was replaced by a set of polynomials representing aspheric corrections. The OS radial profiles are expressed as:

$$z = \frac{cr^2}{1+\sqrt{1-(1+k)c^2r^2}} + \sum \alpha_i r^{2i}$$

Where:

z is the surface profile,

r the surface radial coordinate, ($0 < r < 2154.5$ mm)

c the curvature (the reciprocal of the radius of curvature, radius of curvature = -8223 mm),

k the conical constant ($k = 0$),

α_i the coefficients of the asphere.

As a figure of merit for the optimization of α_i it was requested that the diameter of the circle containing the 80% of focussed light (D80) has to be minimized across the full FoV of 8° degrees.

The polynomial optimization approach follows a method that is similar to the Ritchey-Chretien design since on-axis aberrations are admitted in order to contain off-axis ones. This allows obtaining an angular

resolution almost flat across the entire FoV. CTA-SST polynomial design can hence be considered as a customization of the SC design for Cherenkov telescopes purposes. The optimization has been performed using ZEMAX software for theoretical mirror shape (without taking into account the effects of mirror fabrication and misalignment).

The coefficients to be set in the optical design formula to describe the three OSs are listed in Table 2.

Table 2 – Coefficients to be set in the optical design formula to describe the radial profile of the three OSs.

COEFFICIENT	M1	M2	DET
α_1	0.00	0.00	0.00
α_2	9.61060e-013	1.62076e-011	0.00
α_3	-5.65501e-020	-2.89584e-017	0.00
α_4	6.77984e-027	8.63372e-024	0.00
α_5	3.89558e-033	3.34856e-030	0.00
α_6	5.28038e-040	-1.03361e-036	0.00
α_7	-2.99107e-047	-6.73524e-043	0.00
α_8	-4.39153e-053	-3.06547e-049	0.00
α_9	-6.17433e-060	3.17161e-055	0.00
α_{10}	2.73586e-066	-3.71183e-062	0.00

2.4 M1 description

The radial profile obtained for M1 is reported in Figure 2, as can be observed the concavity of the mirror of about 25 cm and the difference from a sphere is in the order or millimetres.

Given the large diameter the primary mirror was implemented as a segmented mirror following the scheme reported in Figure 3. The full reflector is composed of 18 segments (the central one is not used). The segmentation requires three types of segments having different radial distance by the optical axis and hence different surface profiles:

- Inner corona (segments on the green circle): COR1;
- Central corona (segments on the blue circle): COR2;

- Outer corona (segments on the yellow circle): COR3;

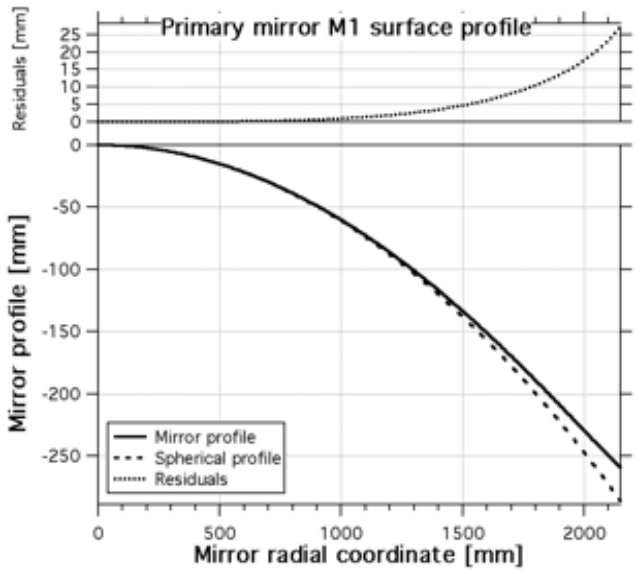

Figure 2 – Profile of M1 as function of the radial coordinate

The 18 segments of the primary mirror of CTA-SST are hexagonal, with vertex-vertex direction along the X axis with aperture equal to 846 mm from face to face. Each segment has at least 6.5 mm of gap from the neighbours for mounting and alignment purposes. Each segment will be equipped with three actuators to correct tilt and piston in alignment phase.

M1 segments are manufactured by cold slumping as sandwiches of glass foils and a structural honeycomb layer with total thickness of 25 mm. 3 interfaces are glued on the back of each segment to interface to the telescope structure. The sandwich structure is then coated on the concave side and finally sealed to be watertight.

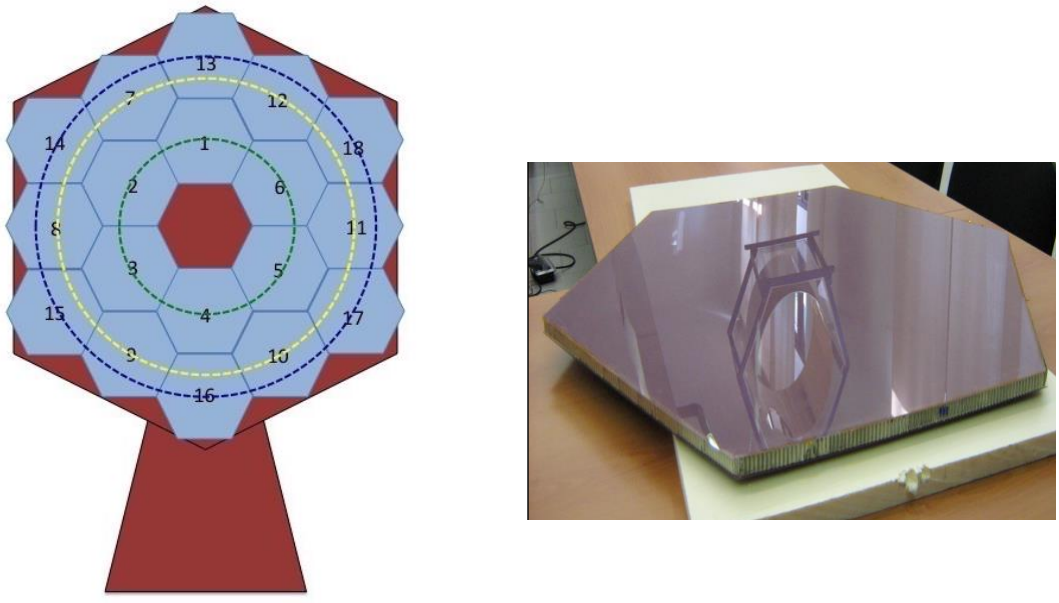

Figure 3 – Left: Sketch of the disposition of the segments of the primary mirror. Right: Picture of uncoated manufactured M1 segment.

Table 3 – Cartesian coordinates of the centres of the M1 segments

Hexagon number	x	y	z
1	856.5	0.0	44.2
2	428.2	741.4	44.2
3	-428.2	741.4	44.2
4	-856.5	0.0	44.2
5	-428.2	-741.4	44.2
6	428.2	-741.4	44.2
7	1280.5	738.8	129.6
8	0.0	1478.6	129.6
9	-1280.5	739.3	129.6
10	-1280.5	-739.3	129.6
11	0.0	-1478.6	129.6
12	1280.5	-739.3	129.6
13	1704.8	0.0	170.6
14	852.4	1476.4	170.6
15	-852.4	1476.4	170.6
16	-1704.8	0.0	170.6
17	-852.4	-1476.4	170.6
18	852.4	-1476.4	170.6

2.5 M2 description

The radial profile obtained for M2 is reported in Figure 4, as can be observed the concavity of the mirror of about 20 cm and the difference from a sphere is in the order of 1 millimetre.

The secondary mirror is a monolithic mirror realised by a hot slumped glass foil 19 mm thick. The curved substrate is then coated on the concave side and equipped with 9 interfaces to the telescope structure (see picture in Figure 5). A hole of 30 mm diameter would be present in correspondence of the mirror vertex to allow camera calibration.

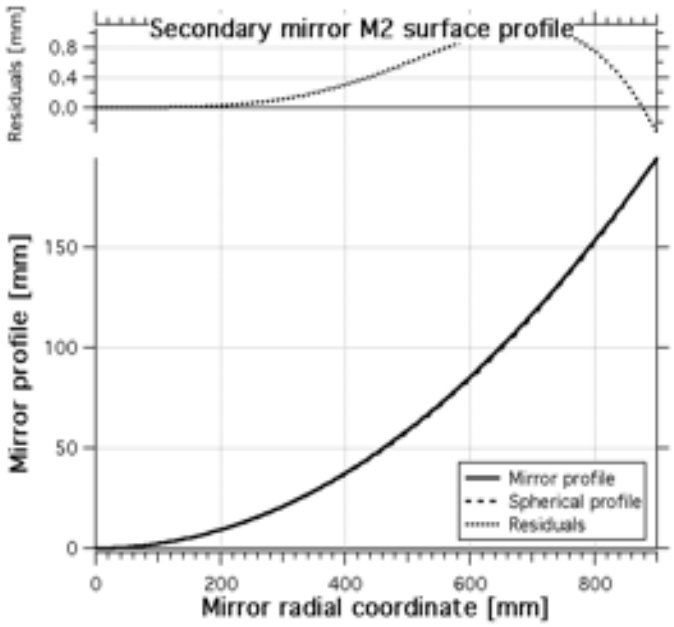

Figure 4 - Profile of M2 as function of the radial coordinate.

Figure 5 – Picture of the back side of a manufactured M2 mirror.

2.6 Coating description

The mirrors reflectivity depends on the mirrors coating that would be based on aluminium coating with protective overcoating capable to reflect >90 % in the wavelength band 300-550 nm. The baseline for CTA-SST protective overcoating is a layering of SiO2 and ZrO2. The proposed CTA-SST coating already underwent accelerated tests to simulate the environmental exposure in lifetime (as required in [AD4]). Moreover, full mirror samples were exposed at CTAO south site for 2 years showing no degradation. The performed tests point out that the CTA-SST mirrors are not expected to loss reflectivity beyond the requirements in lifetime.

2.7 Micro-roughness

It is well known that surface micro-roughness due to optics manufacturing process can degrade the angular resolution by scattering effect. For CTA-SST optics we adopted slumping technique for manufacturing in order to take advantage of commercial glass native smoothness (< 2 nm). Both cold slumping and reverse hot techniques indeed leave the glass smoothness uncorrupted (hot slumping on M2 works on the back plane). In this condition blurring due to glass roughness is negligible wrt the tolerance on slope errors. That is why we just ask to maintain the glass commercial roughness as surface smoothness requirement. As a reference we report here the effect of different roughness values simulated by Fresnel equation (result is analogous to TIS) for sources in the CTA considered energy range [300-550 nm] demonstrating that even for a source of light at 300 nm (Figure 6 left) the loss for a surface with 2 nm micro-roughness is less than 2% while at 550 nm (Figure 6 right) is ~ 1%.

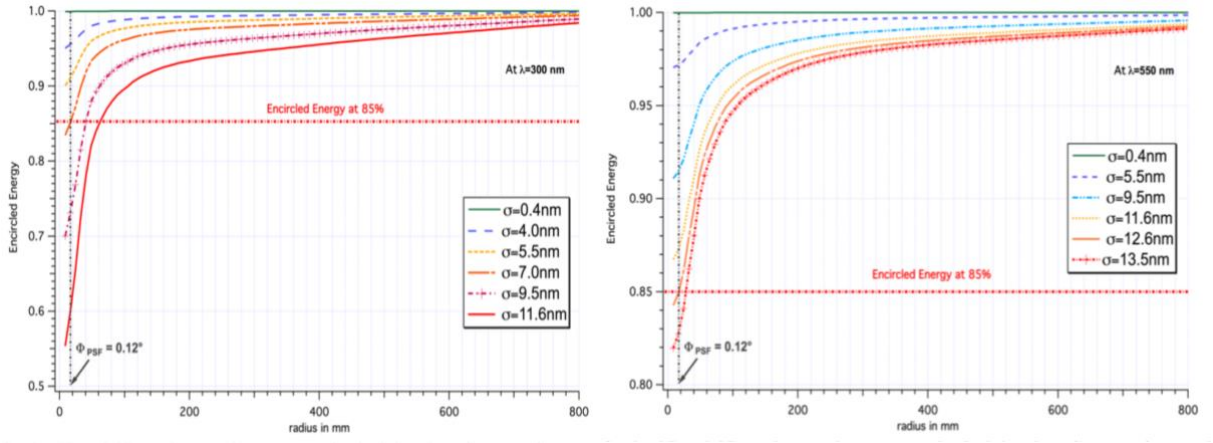

Figure 6 – Effect on EE of different level of surface micro-roughness (Tayabaly et al., Proceedings of the SPIE, Volume 9603, id. 960307 14 pp., 2015).

3 Justification

In this section we report the optical performances of the OS described in the previous paragraphs demonstrating that the chosen design fulfils the telescope technical requirement specification reported in [AD3]. The final telescope OS performance is addressed to other documents considering also the detector characteristics (detailed shape, efficiency, interface window material transmission). All the characteristics reported in this paragraph were obtained by geometrical ray-tracing simulation performed by an IDL tool representing the optical system M1-M2-FS as defined in Table 2.

The simulation code inputs set to obtain the optical performance were:

- Photon density on M1 of 1 photon/cm^2
- Point-like source at a distance of 10 km
- Off-axis angular range 0-5 degrees with steps of 10 arcmin
- Source off-axis direction 0 and 30 degrees (corresponding to the shorter and longer radial coverage of M1)

3.1 D80 requirement

The focal spots generated at the focal plane by the described OS when imaging a point-like source at a distance of 10 km and off-axis angle of at 0°, 1°, 2*, 3°, 4° and 5° degrees are reported in Figure 7.

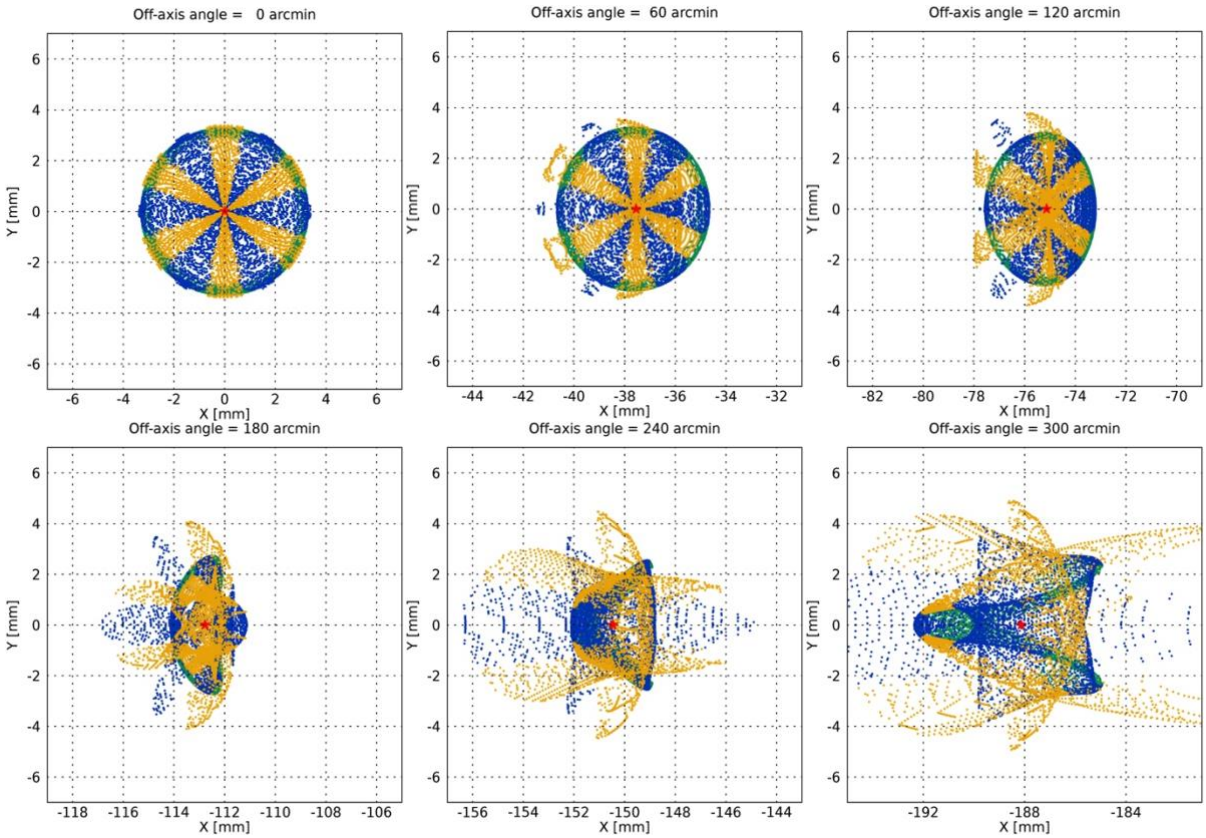

Figure 7 – Focal spots obtained for CTA-SST optical design imaging a point-like source at off-axis angles 0°, 1°, 2, 3°, 4° and 5° degrees. Photons reflected by M1 corona 1, corona 2 and corona 3 are represented in green, blue and yellow respectively. The red star defines the focal spots' barycentre's.*

The images shown in Figure 7 have also been adopted to evaluate the EE curves plotted in Figure 8. As can be seen all the lines, corresponding to on-axis source (black), 1° off-axis (blue), 2° off-axis (cyan), 3° off-axis (green), 4° off-axis (yellow) and 5° off-axis (red) show that the 80% of the photons is always contained in a radial dimension less than 3.5 mm (pixel radial dimension).

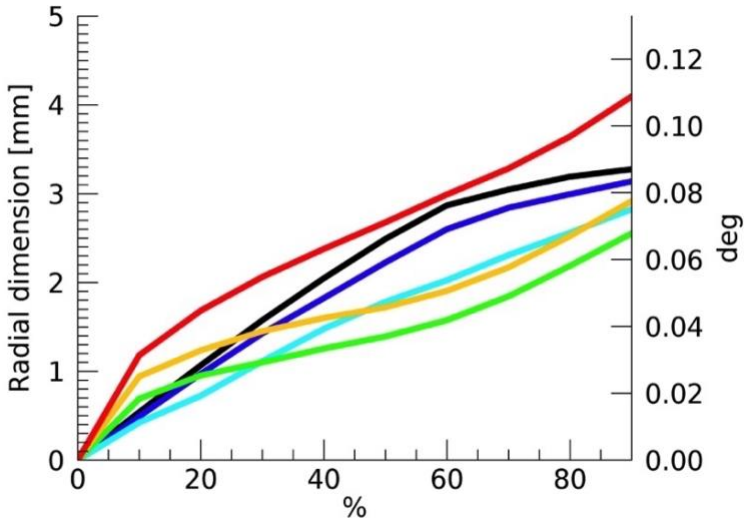

Figure 8 – Encircle energy curves for the focal spots obtained for CTA-SST optical design imaging a point-like source at off-axis angles 0°, 1°, 2°, 3°, 4° and 5° degrees.

The OS D80 across the FOV is shown in Figure 9. It was obtained integrating the PSF in Figure 7 in radial direction with respect to their barycentre until the 80% containment (blue solid line). As can be observed the D80 in contained in a Cherenkov pixel of 7 mm and well below the 0.25° D80 requirement across the full FoV.

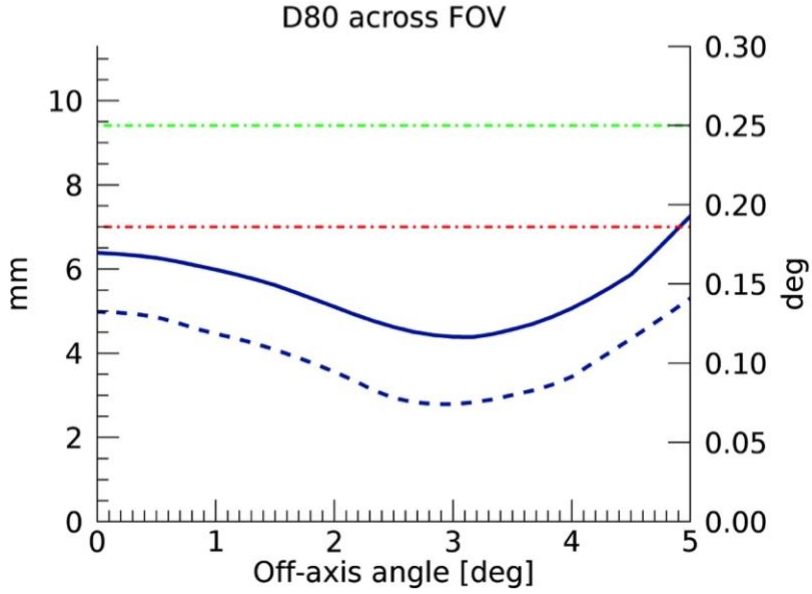

Figure 9 - Solid blue line: D80 across the FoV. Dashed blue line: D50 across the FoV. Red horizontal line: CTA-SST pixel dimension. Green horizontal line: D80 requirement.

3.2 FOV requirement

The OS plate scale was obtained by linear fitting the radial position of the barycentre of the PSFs obtained for sources at different off-axis angles across the FOV (Figure 10). The residuals by the linear fit across the FOV, corresponding to local plate scale fluctuations are reported in Figure 11. The obtained plate scale is 37.643 mm/deg with local fluctuation within 10 arcseconds. Considering the obtained plate scale a FOV of 8° is covered placing at the focal plane a Cherenkov camera with an active area larger than 301 mm in diameter.

The OS equivalent focal length obtained as plate scale / off-axis angle is then 2154 mm with local fluctuation across the FOV in the range 2151 - 2156 mm (Figure 12).

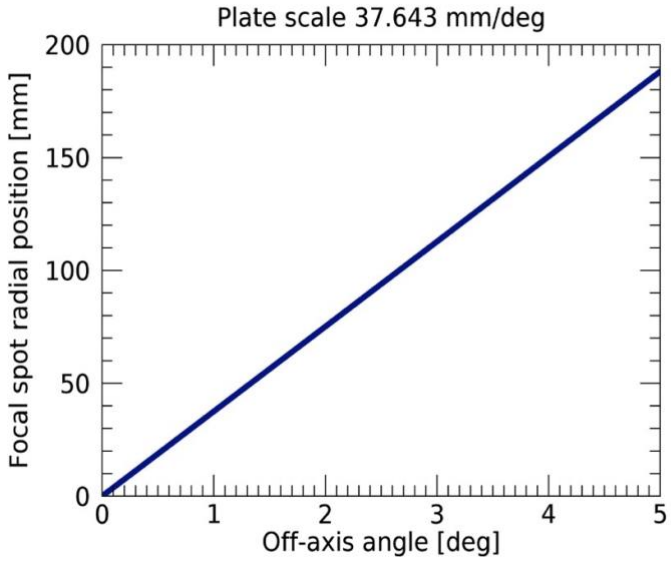

Figure 10 – Dependence on source off-axis position of the radial position of the PSFs barycentre's.

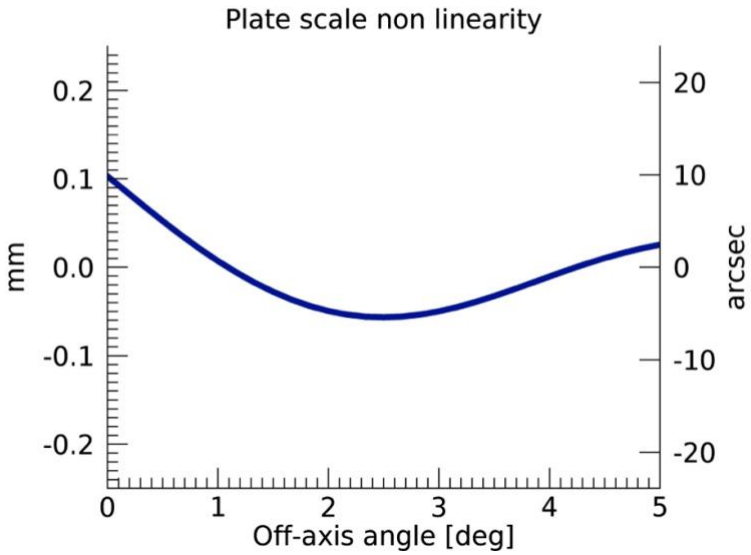

Figure 11 – Plate scale fluctuations across the FOV.

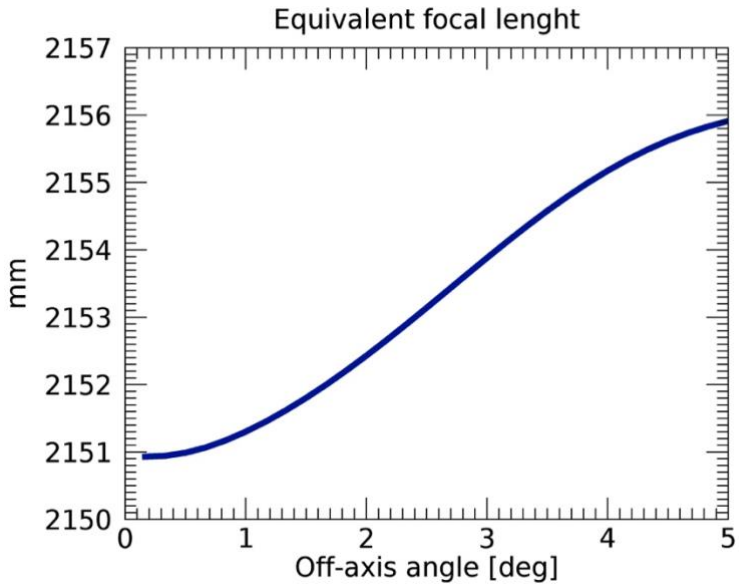

Figure 12 – Equivalent focal length fluctuations across the FOV.

3.3 Isochronocity requirement

The time dispersion of the optical system was obtained considering the PV values of the optical path length across the FOV divided by speed of light. The obtained isochronicity is the range 0.65-1.55 ns (*Figure 14*).

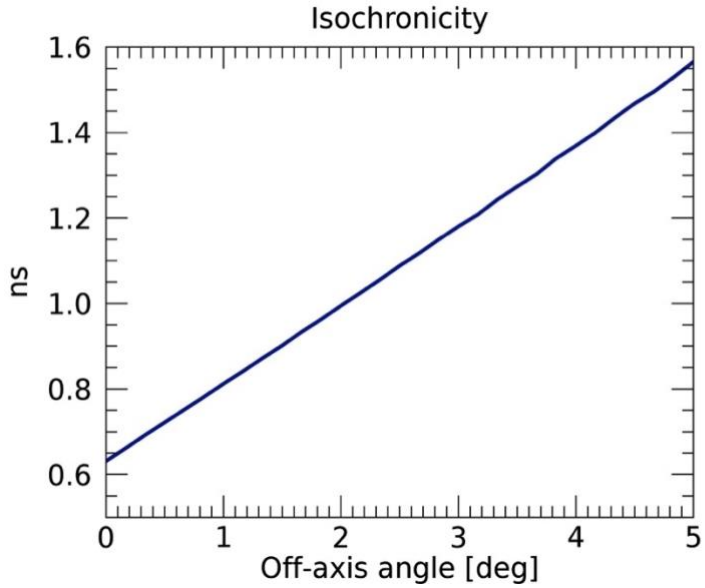

Figure 13 – Isochronicity of the optical system across the FOV.

3.4 Geometric Area Requirement

The geometric area of the CTA-SST telescope was evaluated as the fraction of photons reaching the focal plane with respect to the photons launched on M1 surface normalized to M1 physical area. The geometrical area is dependent on the off-axis angle because of area loss due to shadowing.

In the geometrical area simulation, we considered both the area loss intrinsic to the optical design and the one due to the telescope support structure. In *Figure 14* we report the M1 coverage with colour coded area shadowed by different components, good area is represented in blue while for vignetted areas colour code we refer to the following list. The obtained vignetting contributions and geometrical area values are shown in Figure 15

Contributions to area loss intrinsic to the optical design are:

- M2 shadowing (lilac)
- Fraction of photons reflected by M1 following outside M2 (magenta)

Support structure elements contributing to area loss by shadowing are:

- M2 support structure (yellow)
- Telescope masts (green, cyan and orange)
- Camera case assumed to be a basket of dimension capable to contain the FS (pink and turquoise).

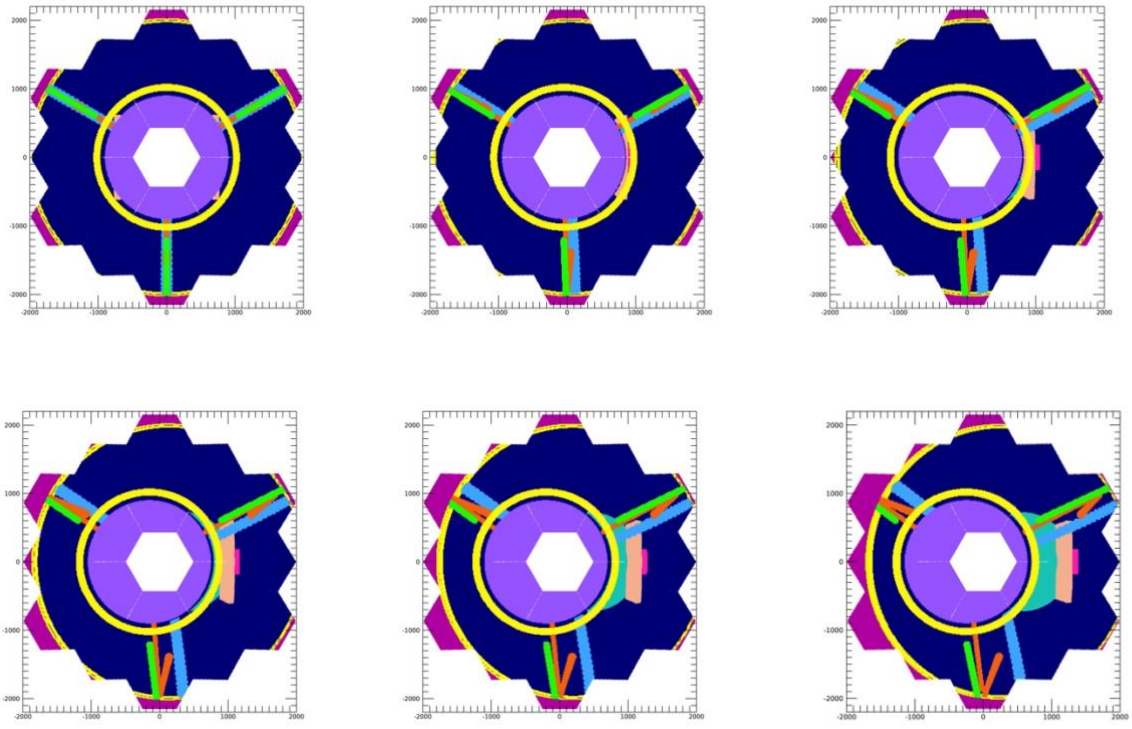

Figure 14 - M1 coverage with color-coded area shadowed by different components, good area is represented in blue while other colours represent the regions vignetted by the different components.

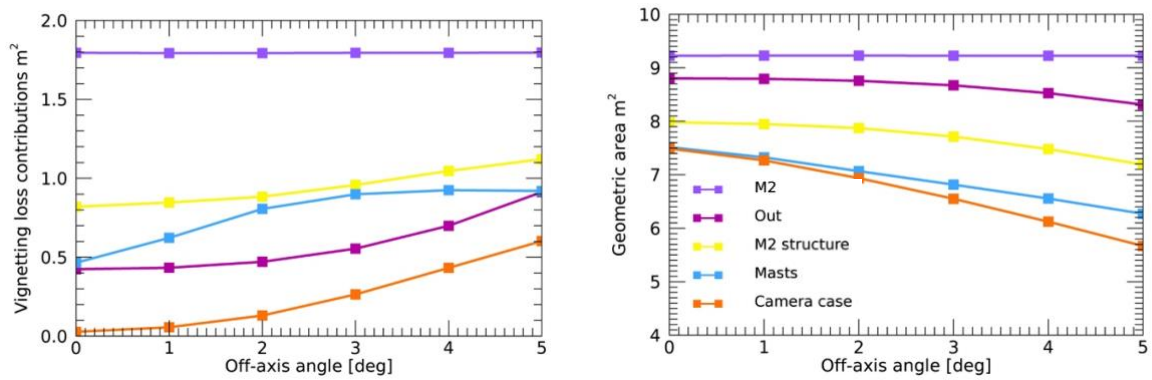

Figure 15 – Left panel: contributions of the different considered components to area loss. Right panel: geometric area obtained by cumulative subtraction of the considered shadowing components.

4 Optical components error budget

Optical components error budget was studied by ray-tracing simulations tolerancing optical misalignments (rotations and translations) and mirrors deformations considering the requirement to maintain the D80 within 1 Cherenkov pixel (7 mm). The study was repeated for M1 and M2 cases to set tolerances to each contribution and then reformulated taking into account the contributions that can be compensated and the ones that cannot.

4.1 M1 segments contributions

M1 segments possible source of optical degradation are:

- Lateral shift: this component has the physical limit of the gaps between the mirrors.
- Focal shift: the effect is different when M1 and M2 are shifted to be closer or farer. Single panels Z translations errors can be compensated by means of panels' pistons and M2 piston within the panels' focal depth. The effect is simulated by random pistons with Gaussian distribution added to the theoretical M1 positions.
- Tilt: The effect is simulated by random angles with Gaussian distribution added to the theoretical M1 tilts. The effect can be compensated by means of panels' actuators within the OC resolution.
- Mirrors shape error: this effect is simulated by random angles with Gaussian distribution added to the theoretical directions of photons reflected by M1. This component cannot be compensated and the translation into height error on panels is completely dependent on the specific spatial frequencies' distribution characterizing the shape error.

The obtained results obtained in terms of D80, EE, and barycentre shifts and PSF aspects are reported in Table 4 and in Figure 16.

	Val	D80 [mm]	D80 [deg]	EE [%]	Xc [mm]	Yc [mm]
	//	5.91	0.15	100	0	0
Lateral shift rms	3 mm	6.83	0.18	87	0	0.2
Focal shift rms	+8 mm	6.97	0.18	84	0	0.1
	- 12 mm	7.11	0.18	83	0.2	0.2
Tilt X/Y	1.9 arcmin	6.85	0.18	90	0.15	0
Rot XY	20 arcmin	7.13	0.18	86	0.1	0.4
RoC	-4 mm	7.14	0.18	91	0	0
	18 mm	6.77	0.18	83	0	0
rms	0.9 arcmin	6.99	0.18	87	0	0

Table 4 – List of considered optical performance degradation contributions to M1 optical performance and relative tolerances to fulfil the D80 requirement.

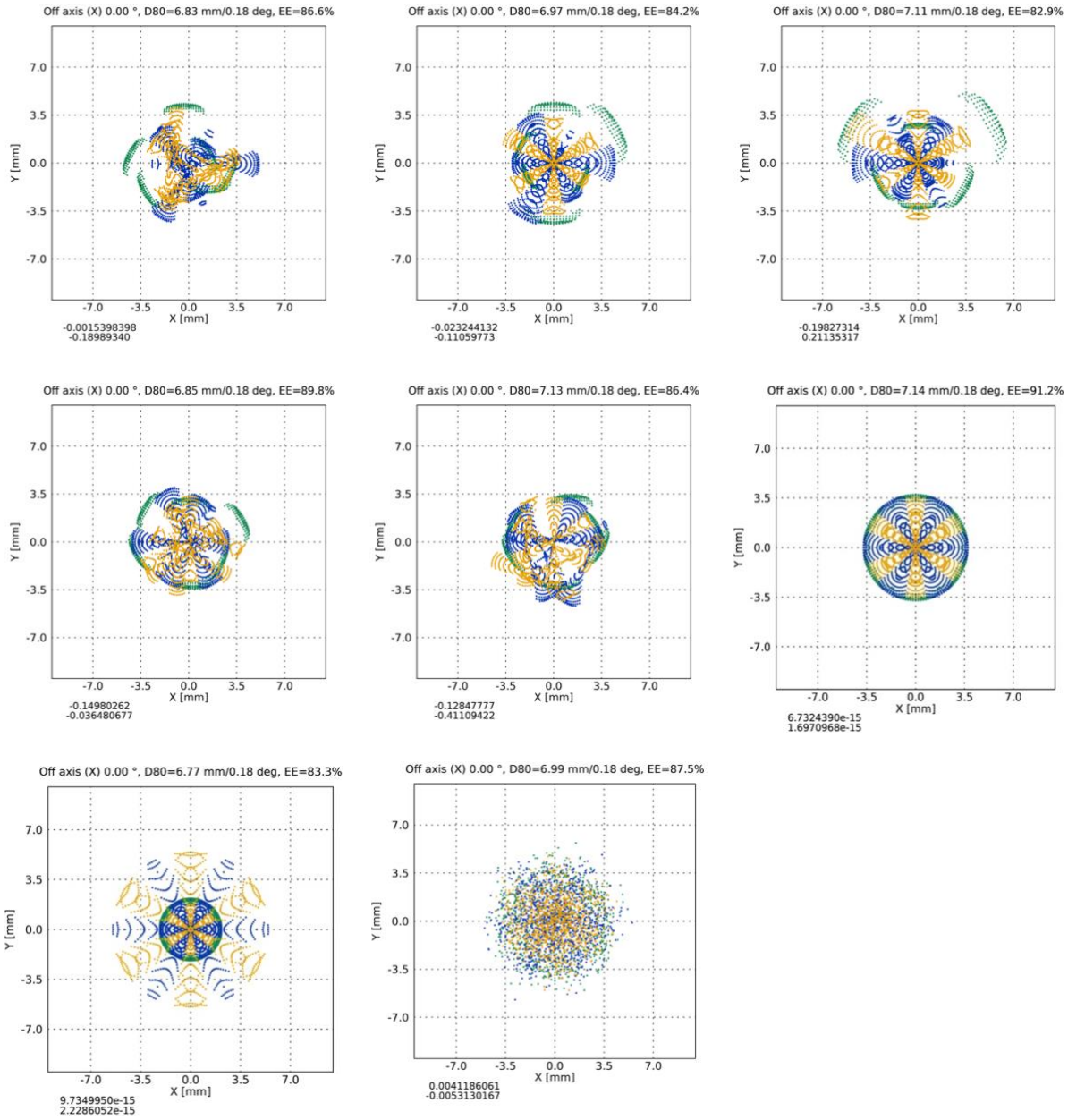

Figure 16 – PSF images obtained for possible degraded modes of M2 listed in Table 4.

4.2 M2 contributions

M2 possible source of optical degradation are:

- Lateral shift: this component has identical behaviour in X and Y directions and can be partially compensated by M1 panels common tilt.
- Focal shift: the effect is different when M1 and M2 are shifted to be closer or farer. The effect can be compensated by M2 piston within the focal depth resolution.
- Tilt: this component has identical behaviour in X and Y directions and can be compensated by M1 panels common tilt.

- Mirror shape error: this effect is simulated by random angles with Gaussian distribution added to the theoretical directions of photons reflected by M2. This component cannot be compensated and the translation into height error on mirrors is completely dependent on the specific spatial frequencies' distribution characterizing the shape error.

The obtained results obtained in terms of D80, EE, and barycentre shifts and PSF aspects are reported in Table 5 and in Figure 17.

	Val	D80 [mm]	D80 [deg]	EE [%]	Xc [mm]	Yc [mm]
	//	5.91	0.15	100	0	0
Lateral shift	6 mm	6.93	0.18	90	1.1	0
Focal shift	1.5 mm	7.01	0.18	82	0	0
	- 0.4 mm	7.04	0.18	93	0	0
Tilt X/Y	6.5 arcmin	6.97	0.19	90	3	0
RoC	-6 mm	6.97	0.18	82	0	0
	+3 mm	7.14	0.18	91	0	0
rms	1.8 arcmin	6.93	0.18	89	0	0

Table 5 – List of considered optical performance degradation contributions to M2 optical performance and relative tolerances to fulfil the D80 requirement.

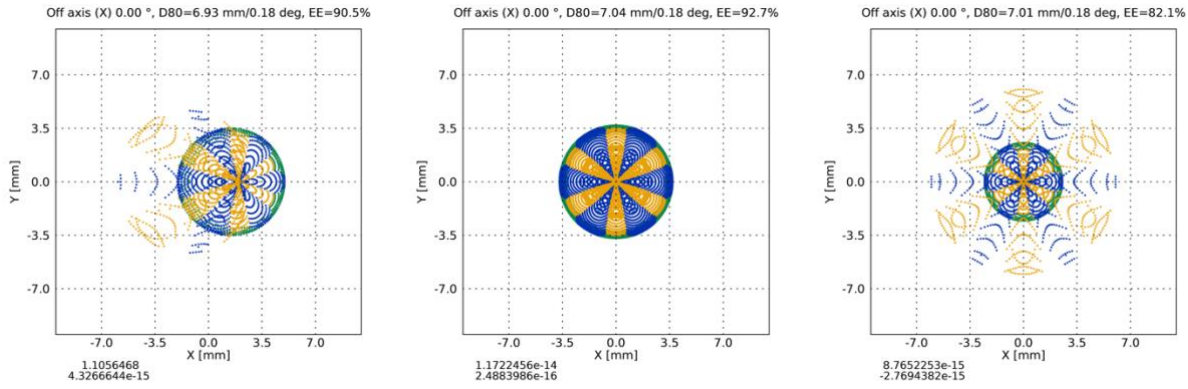

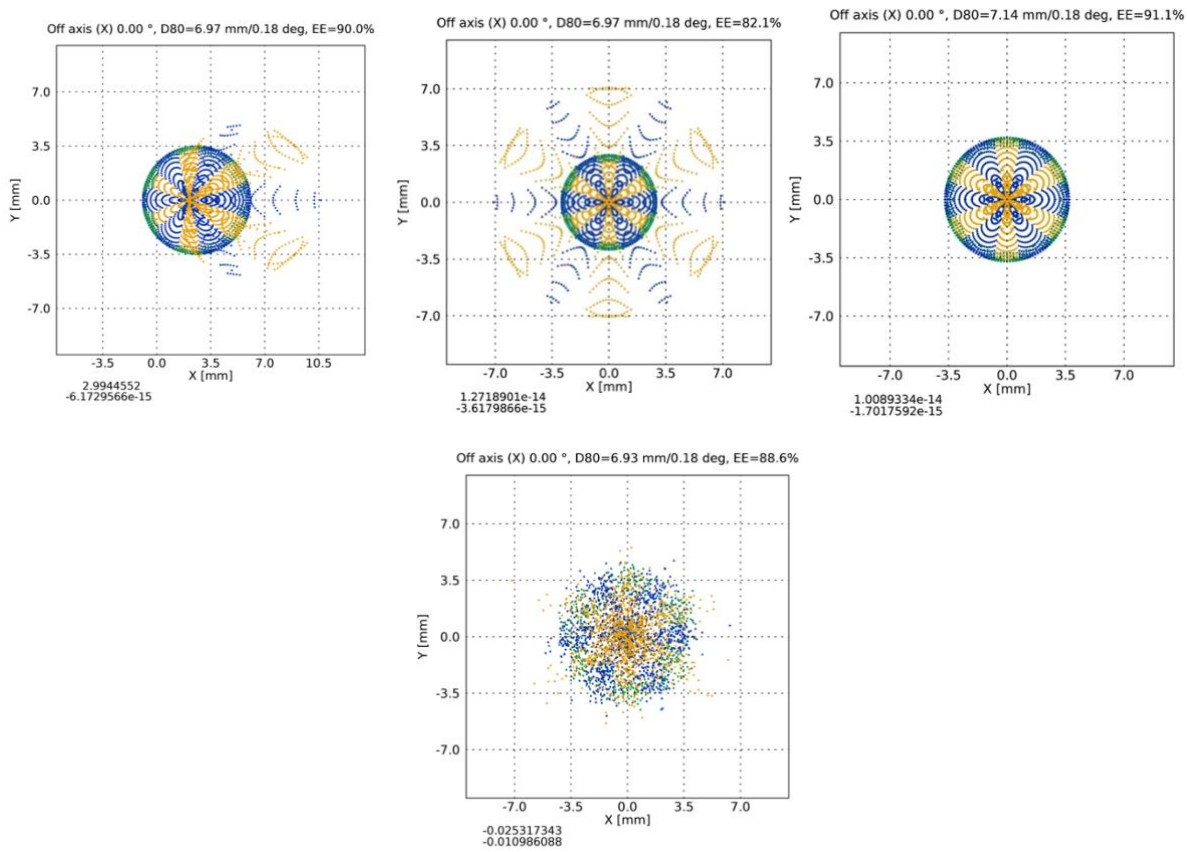

Figure 17 – PSF images obtained for possible degraded modes of M2 listed in

RoC	-6 mm	6.97	0.18	82	0	0
	+3 mm	7.14	0.18	91	0	0
rms	1.8 arcmin	6.93	0.18	89	0	0

Table 5.

4.3 Error budget composition

The composition of the error contribution for the ASTRI OS was studied in three steps considering the different contributions correlations and the possibility to compensate them by means of mirrors actuators in alignment phase.

We can separate the error contributions in the following families:

- Contributions generating PSF diffusion: these contributions are the one related to shape errors of the mirrors. These contributions shall be studied taking into account the specific spatial frequencies distribution of the shape errors since uniform diffusion and local accumulation points give different results.

  The effect of rms errors on M1 and M2 is uncorrelated and the composition of the rms values indicated in Table 4 and Table 5 gives a still in specification result across the full FoV.

	Val	D80 [mm]	D80 [deg]	EE [%]	Xc [mm]	Yc [mm]
Rms M1	0.9 armin	7.07	0.18	87	0	0
Rms M2	1.8 arcmin					

Table 6 – Results of the composition of shape errors of M1 and M2.

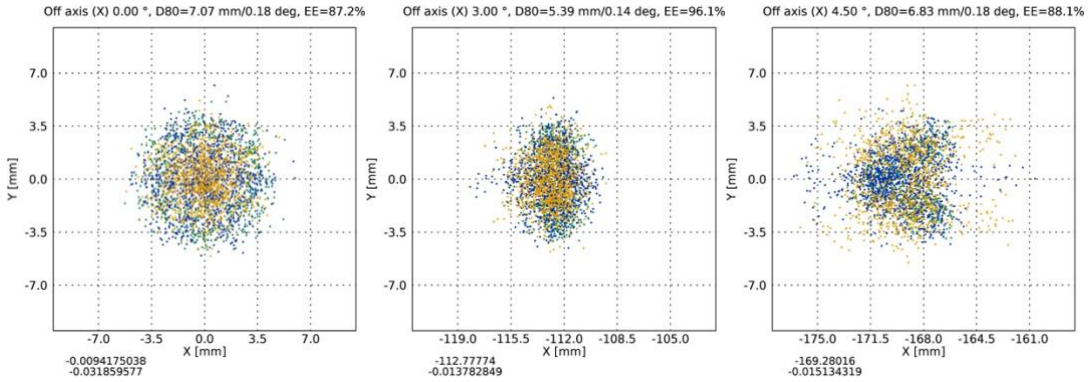

Figure 18 – PSF on-axis, at 3° and 4.5° off-axis obtained for the composition of shape errors of M1 and M2.

Considering the nowadays-available information about the manufacturing process by replica and the moulds shape error we also performed tests and simulations on already available materials demonstrating that the specification can be relaxed thanks to the absence of high spatial frequency errors.

- Contribution changing the OS focal length: these are the RoC errors of M1 and M2 and the focal shifts. These terms are correlated and can be compensated by M1 single panels pistons and M2 global piston. As a result, the tolerance on M1 and M2 RoC errors is driven by the dynamical range of the M1 and M2 actuators that is 15 mm. This means that for M2 the RoC error can be even larger than the one computed by simulations.
  Moreover, the defocusing was considered in the simulation as a whole while this can be compensated in alignment adding tilts to the mirrors. As an example, we report the simulated PSF of a perfect OS with M2 defocused by 2 mm giving an out of spec result in terms of EE. By the way, as can be observed in Figure 19, all the PSFs generated by the single panels fit the pixel dimension (red square) and can be moved one by one inside the pixel tilting the mirrors to obtain a non-continuous surface. The study on single panels tolerances considering the realignment was performed both of simulated and measured data and the result used as specification requirement for M1 segments production. The study demonstrated that even when a single PSF is really out- of spec (50 mm RoC error and EE on axis degraded to 76 %) the composition of the 6 segments generates an in-spec corona (EE 86%)

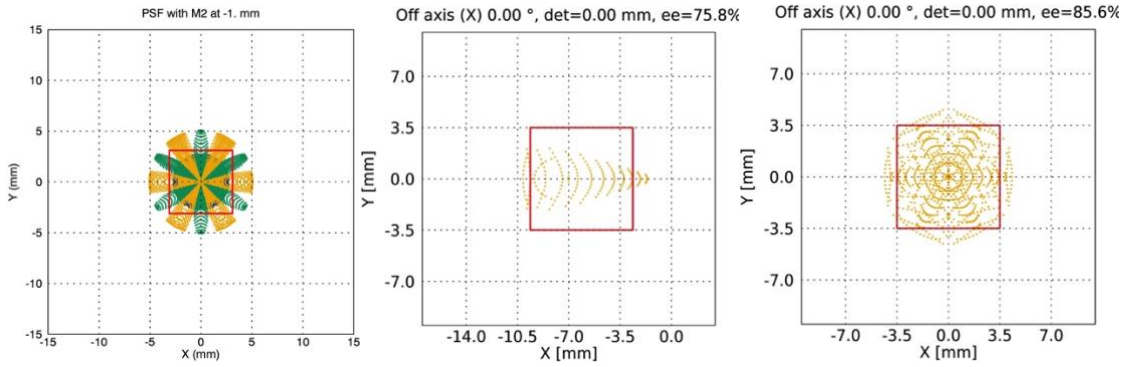

Figure 19 – PSF images obtained for M2 shifted by 2 mm. Left: full PSF with no realignment. Centre: PSF of a single panel with RoC error of 50 mm. Right: PSF of the whole corona.

- Contribution changing the PSF barycentre: they are the lateral shifts, XY tilts and rotations. All these contributions act shifting the PSF barycentre at a whole (if M2 is considered) or segment by segment (if M1 is considered). These contributions are uncorrelated and the assigned tolerances can be divided by sqrt (N), where N=8 is the number of considered contributions, to fulfil the requirement.
  Anyway, we point out that all these contributions can be compensated tilting M2 and M1 segments to bring back the single spots in their nominal positions in alignment phase (Figure 20). This means that the tolerance to be taken into account this contribution to the error budget is assessed by the repeatability and accuracy of the mirrors active motion system and the actuators accuracy is by design 30'', quite below the computed tolerance.

	Val	D80 [mm]	D80 [deg]	EE [%]	Xc [mm]	Yc [mm]
Shift M1 rms	1 mm	6.67	0.17	93	1.4	1
Shift M2	2 mm					
Tilt X/Y M1 rms	0.6 arcmin					
Rot XY M1 rms	7 mm					
Tilt M2	2 arcmin					

Table 7 – Results of the composition of errors of M1 and M2.

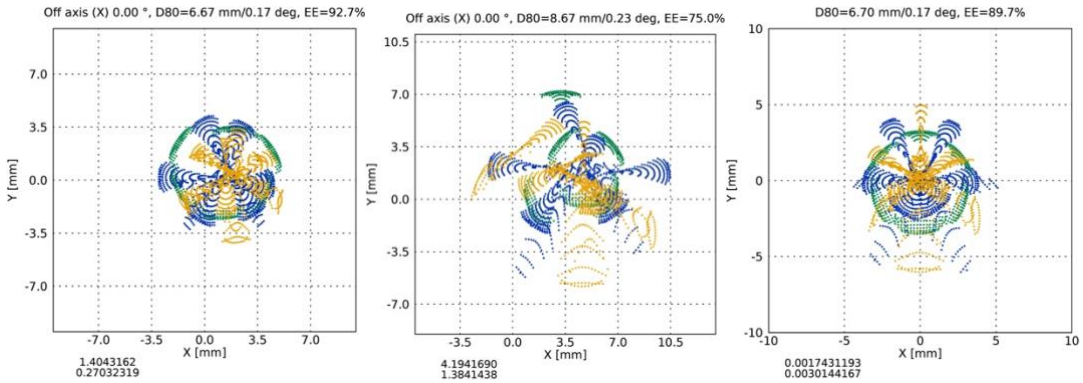

Figure 20 – PSF images obtained for M1 and M2 shifted by 2 mm. Left: full PSF with no realignment. Centre: PSF of a single panel with RoC error of 50 mm. Right: PSF of the whole corona.

End of the document